Challenging best knowledge to real conditions on the SEMREV marine test site

Yves Perignon[#1], Izan Le Crom[#2]

[#]*Ecole Centrale de Nantes, LHEAA Lab. (ECN/CNRS)*
Nantes, France

[1]yves.perignon@ec-nantes.fr
[2]izan.le-crom@ec-nantes.fr

Abstract— **This paper presents a review of the last six years of sea states measurements at the SEMREV test site, compared to latest capabilities in term of wave modelling in a macro-tidal coastal environment [Tolman et al. (2014), Ardhuin et al. (2012)]. This work takes advantage of the HOMERE high-resolution hindcast data set [Boudiere et al. (2013)] for long term analysis, as well as an in house modelling chain based on a similar approach for more specific requirements over the measurement period. The grid refinement is led by a local unstructured mesh and an appropriate coupling and nesting from global to local scales. The retrieval of astronomic tidal harmonics at grid nodes from a one-year high resolution hydrodynamic coastal modelling over the area [Pineau-Guillou et al. (2013)] enables to force at low computational cost both levels and currents impacting the advection of the wave components in the sea state model. The paper provides a brief overview of the properties of the site inferred from the measurement and model capabilities, including the scores of both hindcast chains, the influence of the tidal forcing over the modelling and measurements or the spatial variability on site,**

A special attention is paid in this study to the series of storms striking during winter 2014. The return period of the several singular events is checked against the previously estimated extrapolation method at SEMREV [Le Crom et al. (2013)], as well as the return period of this whole sequence of severe conditions. One of the severe event, significant by the combination of high Hs and long period, is specifically analysed in term of 1 and 2D spectral distributions. This overall demonstrates the capabilities of a fully archived hindcast dataset associated to the latest and more physical accounting for source terms.

Keywords— **Marine test site, sea states, measurements, modelling, extreme conditions, spectral distribution.**

I. Introduction

With the growing interest in the deployment of energy devices in coastal regions for their wind and wave resources, the need for environmental data seems to have grown exponentially. Refine climatology of wave data are indeed of great interest when studying specific requirements in term of ocean engineering: from power resource for any wave energy device, to the loads and fatigue on structures and mooring, or the operability of any given region. In this context, numerical wave models have been used extensively to cope with sparse, rare, expensive and site-specific long term in situ measurements.

Forced or coupled with atmospheric models, spectral 3rd generation wave model are generally able to provide time series of integral parameters with offshore errors less than 20% for significant wave heights and peak periods [Dodet et al., 2010]. Among other sensitivities, the accuracy of a dataset is often evaluated by the grid resolution in space and time of the underlying model. Many other specificities of the model chain also play a key role in the global accuracy of the data set and its sensitivity is greatly site dependant. The forcing and boundary conditions (eg. wind, ice coverage, bathymetry, water lever, current, etc.) are crucial environment parameters, which matter for instance at various extents in the life of waves and sea states. The numerical model itself, as a core enabling proper integration and resolution of the physics, provides another clear link to accuracy. Final but not least, the spectral parameterizations of the physics still remain the main challenge; the time and efforts at stake in the generation of a complete data set can however prevent the latest findings and breakthrough to be included on a regular basis in the latest databases for wave hindcasts.

Many hindcasts, with varying resolutions, coverage, physics, forcing, etc. are available to this date. If the scores related to the performances of their simulations are most of the time expressed in term of errors related to time series of integral parameters, compared to reference data from sensors (in situ as well as remote sensors), the models themselves are based on the spectral description of the sea states. The best description of the model computations is accordingly achieved through the evolution of the full 2D spectra in frequency and direction. Yet, existing hindcasts provide a limited number of parameters, and really few datasets provide such full spectral description (e.g. full spectrum archived at ECMWF).

To our knowledge, the recent hindcast databases issued by Ifremer (IOWAGA project and HOMERE database [Boudiere et al. 2013]) are the only one providing times series of full spectra, with the most complete forcing and boundary conditions, the most up do date parameterizations of the physics [Ardhuin et al., 2009a & 2010] and numerical scheme [Roland et al., 2008 & 2009], providing the best offshore scores. From the SEMREV marine test site point of view this provides the best available knowledge of its wavy environment. The aim of this paper is to challenge the description provided by the model chains to the data collected

at sea since the beginning of the operational phase at Semrev test site in 2009.

More over, HOMERE's data set being computed for the past 1994-2012 period, there is a need for a regular update of the data set. A similar approach to HOMERE model chain is then followed for the setup of a specific hindcast chain dedicated to the SEMREV test site [Saulnier et al. 2013]. The performances of both hindcast chains are evaluated comparatively to the measurements for their common periods.

II. HOMERE HINDCAST

The reader is referred to HOMERE's documentation and reference publications for the full description of the setup. For the sake of clarity, we will only recall its main properties. WaveWatch3 is run in its version 4.09 for the generation of this dataset. HOMERE's domain extends well beyond the regional area related to SEMREV's test site, as it is dedicated to the whole French Atlantic coastal area from the North Sea to the south of the bay of Biscay. An unstructured grid is build up from triangular mesh over the whole domain. A high-resolution bathymetric database (100 and 500m Digital Terrain Model) provides the reference water depth. Offshore wave conditions are inputted from IOWAGA's global runs over the North Atlantic region. The source terms related to wind input, whitecapping, swell dissipation, and wave breaking are based on Ardhuin et al. (2009a, 2010) formulations (source terms ST4 in WaveWatch3 v4.18). The non-linear transfers are modelled thanks to the Discrete Interaction Approximation [Hasselmann et al., 1985]. A specific treatment of the bottom friction accounts for the nature of the bottom and for the coupling between sea states and moveable sediments, and coastal reflection is parameterized through a variable reflection coefficient. The spectra are discretised and solved on a 24 directions and 32 frequencies grid.

Wind conditions are forced by the 6 hourly CFSR NCEP dataset [Saha et al., 2010]. Water levels and currents are accounted by tidal constituent inferred from the harmonic analysis of a one-year period (year 2008) hindcast dataset from a multi-rank MARS 2D circulation chain [Pineau-Guillou et al. (2013)].

The usual scores are of interest on the SEMREV test site, in terms of the comparisons of the hindcast data to the measurements by the sensors on site. Wave conditions on the SEM-REV test site have been continuously monitored (Fig. 1) since 2009 thanks to two directional Datawell MkIII buoys located at either side of the area (East/West, ~35m LAT). A third additional Datawell buoy located off shore Belle-Ile Island provides regional up wave conditions (about 40 km from Semrev test site) in deeper water (~65m LAT). The data traditionally consist in time-series of buoy motions (heave and horizontal motions) sampled at 1.28Hz, from which an estimate of the wave spectrum can be derived over a half-hour or hour period. Here, hourly directional wave spectra are estimated (using FFT and maximum entropy method (MEM)) and integrated over directions with resolution 0.01Hz (0.063rad.s^{-1}).

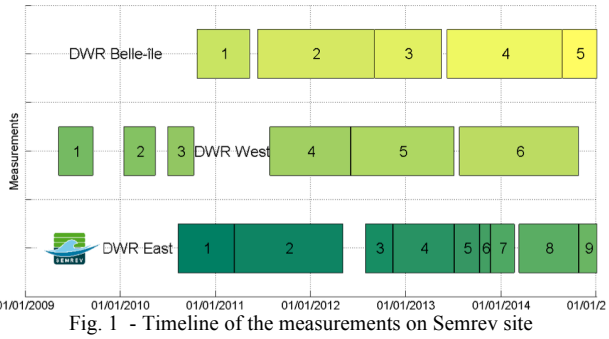

Fig. 1 - Timeline of the measurements on Semrev site

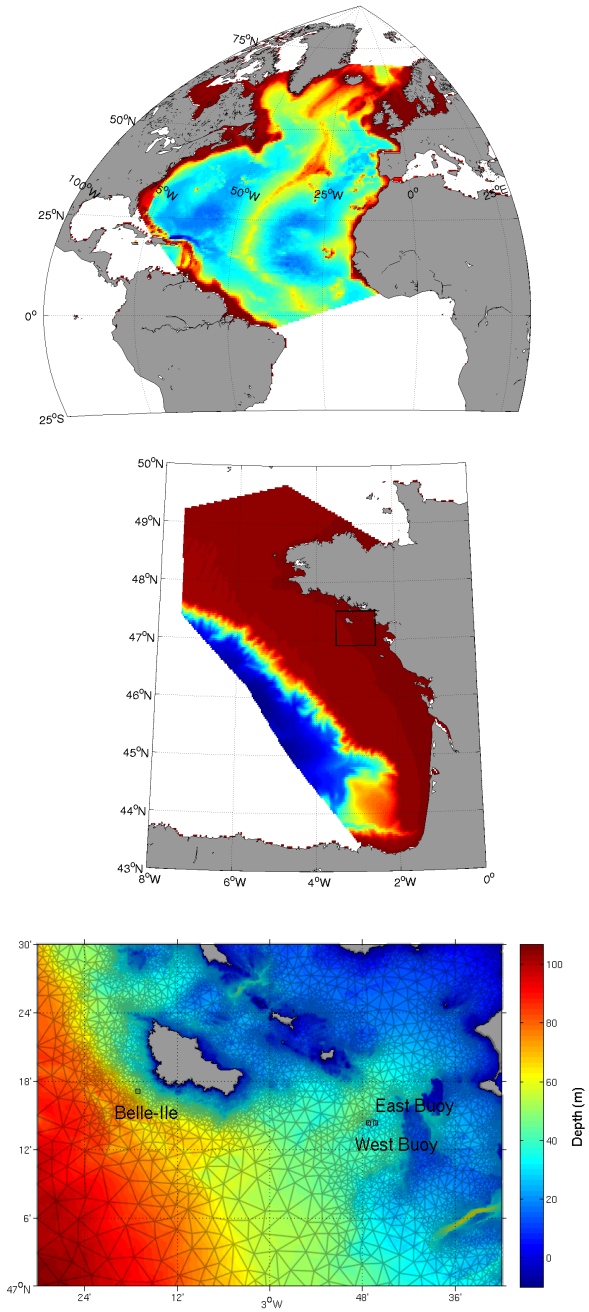

Fig. 2 - Extent of the domains for rank 0, 1 and 2 of the SEMREV in-house WaveWatch 3 model chain.

III. SEMREV IN HOUSE HINDCAST

Due to the fixed duration and parameterizations of HOMERE data set (1994-2012) a complementary set up is built on the same tools with the specific aim to model SEMREV's region (Fig. 2). Three ranks are defined, from a global 0.5° regularly arc gridded domain at the scale of the north Atlantic basin, coupled to a regional regular grid over the Biscay bay (30' arc resolution), both forcing a local irregular grid with element sizes from about 2 km to 100m. The last irregular rank is forced with level and current fields on the same methodology described in the HOMERE section. Wind conditions for all three ranks are here forced by the 6-hourly ERA-INTERIM ECMWF data set [Berrisford et al., 2011]. Ice Coverage, despite its potential low impact on our region [Dodet et al. 2010] is taken into account in rank 0 global domain by data from the same ERA-INTERIM dataset. The chain has been run from 2010 to the latest available ERA data (about 4 months delay to present time). The location of output related to the positions of the buoys, or more generally to positions of interest, are prescribed to the model, which provides spectra, and associated integral parameters at those prescribed exact locations.

IV. PERFORMANCES AND SITE PROPERTIES

The model results are first discussed here in term of wave height. The errors are expressed in terms of a normal root mean square error (NRMSE)

$$NRMSE(X) = \sqrt{\frac{\sum (X_{obs} - X_{\mathrm{mod}})^2}{\sum X_{obs}^2}} \quad (1),$$

a normalized bias

$$NB(X) = \frac{\sum (X_{obs} - X_{\mathrm{mod}})}{\sum X_{obs}} \quad (2),$$

the Pearson correlation coefficient

$$r(X) = \frac{\sum (X_{obs} - \bar{X}_{obs})(X_{\mathrm{mod}} - \bar{X}_{\mathrm{mod}})}{\sqrt{\sum (X_{obs} - \bar{X}_{obs})^2 (X_{\mathrm{mod}} - \bar{X}_{\mathrm{mod}})^2}} \quad (3),$$

and a scatter index (S.I.) correcting NRMSE from its bias

$$SI(X) = \sqrt{\frac{\sum \left[(X_{obs} - \bar{X}_{obs}) - (X_{\mathrm{mod}} - \bar{X}_{\mathrm{mod}}) \right]^2}{\sum X_{obs}^2}} \quad (4).$$

The comparisons are conducted from 2010 to 2012, over the periods of operational measurements for the individual sensors (Fig. 3).

The best scores are commonly obtained by the models at the most offshore measurement site (Belle-Île buoy) where processes are less impacted by the complexity of more coastal physics to be solved on site at East and West buoys. Despite the relative proximity between east and west buoys (separated by about 1000 m), both models show lower scores at east buoys compared to west buoy.

HOMERE hindcast dataset performs slightly better for all three sites, scatter index S.I. ranging from 11.7% to 14.3% for HOMERE and 14.3 to 15.5% for the in-house model, in term of significant wave height H_{m0} (or H_s in the following). There

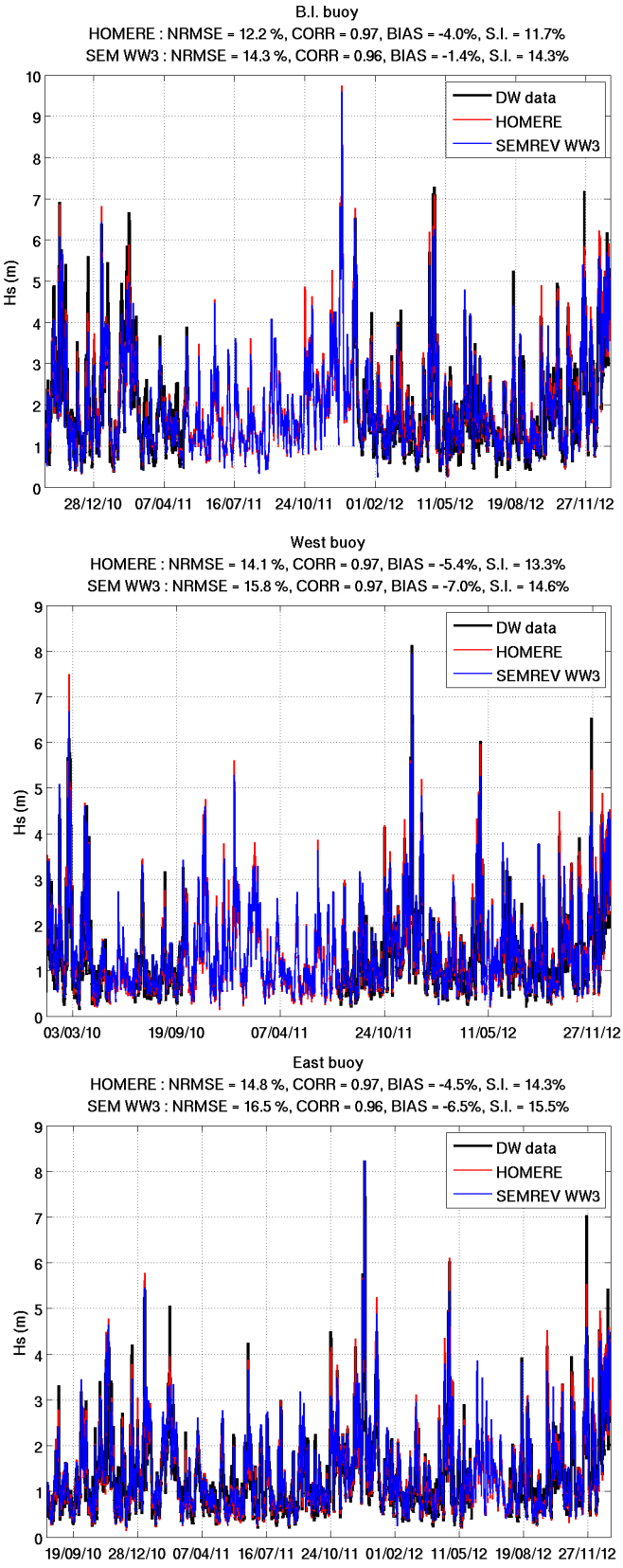

Fig. 3 - Comparisons of significant wave height at Belle-Île, Semrev West and East buoys from 2010 to 2012

are several possible factors which could explain the best scores for HOMERE : the wind forcing is different for both chains, even if the parameterizations are specific to the wind sources [Rascle et al., 2010], the refined irregular grids and associated tidal forcing have different extensions of domains, and the treatment of the moveable bottom parameterization is not equivalent in both chains. Indeed, this parameterization requires a definition of the type of sediment over a domain, which is for now accounted homogeneously in SEMREV's in house chain and heterogeneously in HOMERE. The evaluation of the sensitivities can be a never-ending tasks, but a first evaluation for some processes of interest has however been conducted. Following Ardhuin et al. (2012) evaluation of the impact of the macro tidal environment for a not so distant area (i.e. Iroise Sea), the same evaluation is provided here. Year 2010 is run with and without tidal forcing and a comparison based on the same scores is made on the three measurement sites. An example is provided here during spring tides at West buoy (sept. 2010, Fig. 4). If a semidiurnal tidal modulation can be observed in the measured and modelled data, the natural variability seems to be of the same order of magnitude as the tide modulation. None of the of the tidally forced hindcast in SEMREV's region shows a significant increase in correlation to the measured data. The scores in NRMSE or S.I are slightly improved in strong tide conditions but overall not of a great amount. HOMERE is hardly correlated to the measured fluctuations, and Semrev in-house model with tidal accounting, if better correlated to the measurements, shows a more important bias than the others which impacts its NRMSE. The S.I., correcting the bias, shows the overall better performance of Semrev model when accounting for the tidal forcing. A better accounting of the dissipation term related to the parameterization of the movable bottom friction could be a first lead for a correction of the higher bias in Semrev's model. Ardhuin et al. had shown that the tidal currents and associated strong jets ($U_{\max} \sim 3m.s^{-1}$, from Pineau-Guillou et al.) between islands, up-wave of a measurement site, could be responsible for a great variability in the sea states conditions (variation up to than 40% of Hs bewteen non-tidally and tidally forced wave models). Here, currents between Belle-Ile Island and Quiberon, Houat or Hoedic Islands don't seem able to provide equivalent strong forcing conditions upwave of SEMREV's area ($U_{\max} \sim 1m.s^{-1}$ from the same dataset) and the local variability doesn't exceed 10%.

The relatively low resolution in time (6 hours) in the wind forcing data remains another possible candidate for the lower variability in the modelled data compared to the measurements. The Semrev site being located more than 10km offshore, it is quite exposed in any direction to a local wind sea. Further analysis would benefit from refined temporal data in order to carry out a sensitivity analysis on this aspect.Taking advantage of the close mooring related to west and east wave buoy measurements (about 1000m apart, neglecting the mooring length and associated displacement of the buoys), we are able to provide a first quantitative assessment of the spatial variability on the Semrev test site. The local unstructured grid capability of the model is particularly useful when addressing this specific question: the local grid refinement is either related to the local bathymetric conditions and associated CFL criteria, or to a user prescribed area of interest. The surrounding Semrev area is accordingly refined with a 100m criterion, ensuring about 10 grid points along each dimension in the Semrev in house model. In order to take fully advantage of the not-so-common nearly 5-year synchronised measurements at West and East Semrev's buoys, the comparison is conducted on the equivalent duration in the model chain, that is the in-house model.

A linear first order regression is performed as a first assessment of the trend between both buoy measurements (Fig. 5). The pattern expressed through this linear fit is quite properly reproduced by the inter comparison of the modelled data at East and West locations. More over, the model is able

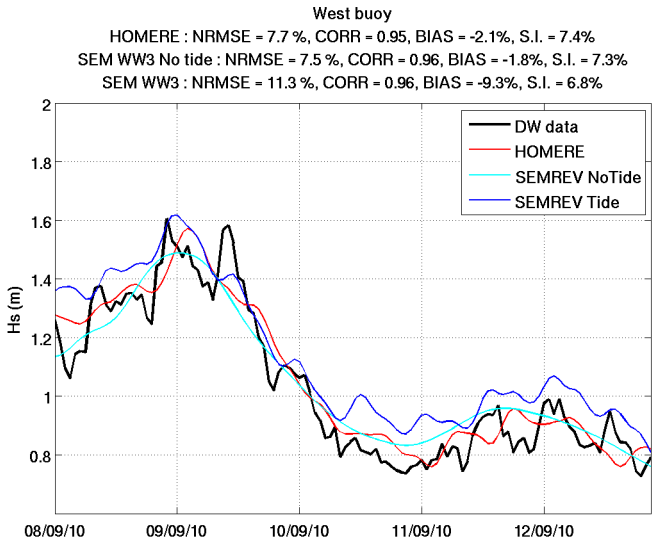

Fig. 4 - Influence of tidal forcing during spring tide on H_s at SEMREV's West buoy

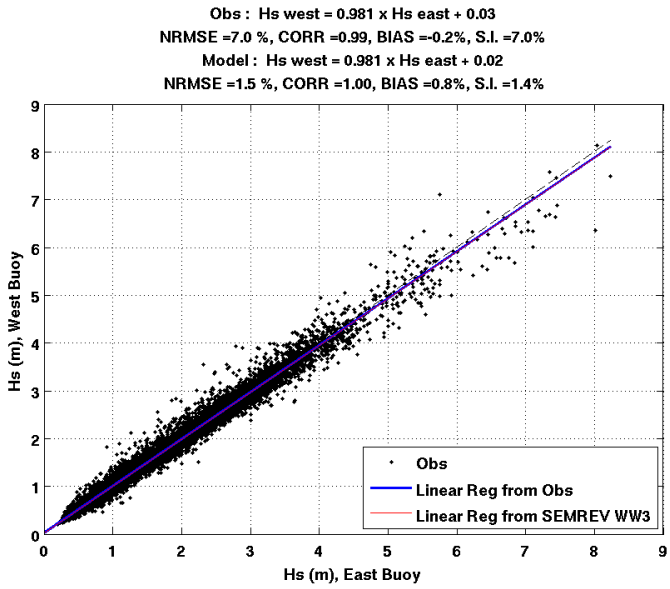

Fig. 5 - Inner-site comparisons, East against West Semrev's buoys

to physically relate nearly 1.5% of the spatial differences over the 7.0% observed between both buoys (both NRMSE or S.I.). All in all, a large part of the natural variability, either product of a sampling artefact or unresolved physical processes (2nd order non linearities such as 3 wave interactions, or bound waves, phase related processes, etc.) cannot be accounted by a numerical modelling approach. More over, a significant part of the discrepancies between synchronized measurements seems to be related to severe conditions. A stronger quality check of the measurements, as well as a better understanding of the motion of the moored buoy in strongly whitecapping conditions could most probably significantly enlighten the recorded spatial variability.

V. Extreme Events

From the previously described dataset, it can be of interest to infer return periods for the extreme events, and associated long-term extrapolations. The HOMERE data set is extended by the 2 complementary years from Semrev's in house modelling chain. The same methodology as in Le Crom et al. (2013) is followed here updating the findings with more accurate hindcasts. A Peak Over Threshold (POT) analysis associated to a declusturing procedure (i.e. separation criterion in time) aims to provide a proper sampling of the tail of the parameter distribution. A General Pareto Distribution (GPD) is fitted to this sampling, and combined to a Poisson distribution enabling the evaluation of the value of the parameter for a given return period (Fig. 6). Such estimation for the return period in term of H_s is of great interest for common ocean-engineering dimensioning processes. For the estimate at East buoy, the parameters of the best fit are given by the GPD distribution function following

$$F(x;k,\sigma)=1-\left(1-kx/\sigma\right)^{1/k}, \quad k=0.0557, \quad \sigma=1.0220, \quad x\geq 5m \qquad (5).$$

The threshold is deduced from the same convergence analysis provided in Le Crom et al., in order to guarantee the most conservative evaluation of the fit.

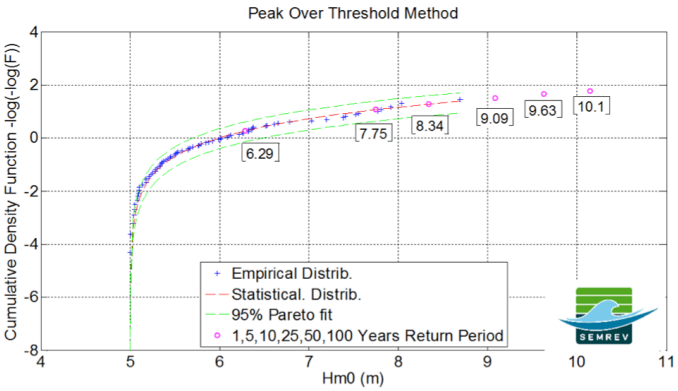

Fig. 6 - Extreme value analysis: POT method and GPD best fit applied to East Buoy analysis at Semrev's test site.

The response of a structure at sea, in term of motion or loading, being specific by nature, there is a great interest in taking advantage of the 2D spectral description provided by HOMERE or Semrev in-house dataset. There is however a great challenge in the definition of design processes without inferring joint probability laws, which would impair the realism of the forcing conditions. Thilleul et al. (2014) have illustrated the promising results in the combination of Response Based Design methods providing a first sensitivity analysis of the structure (e.g. I-FORM method), to past scenarios from hindcast and appropriate extrapolations, which would be considered as dimensioning cases.

A special attention is then paid to the conditions occurring during winter 2013-2014, the sequence of sea state is the most severe since winter 1989-1990, according to a quick review of the storm intensities and durations from integral parameters in IOWAGA North-East Atlantic 24-year dataset. It is then quite noticeable that from December 10th 2013 to March 10th 2014, the significant wave height on site has not decreased below $H_s = 1m$ during 90 days, except for one short window, less than 24h between January 10th and 11th (Fig. 7). One should

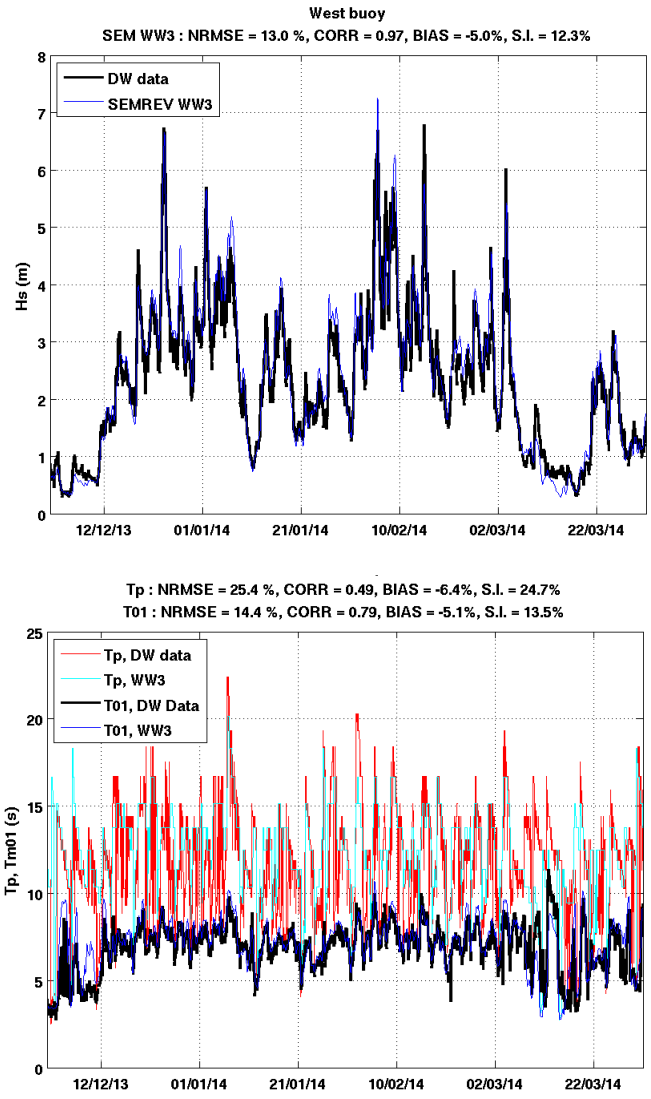

Fig. 7 - Evolution of measured and modelled integral parameters H_s, T_p and T_{m01} over the winter 2013-2014 at West buoy on Semrev site

emphasize the overall performances of the model, with remarkably good scores for a sequence of severe sea states, which should challenge most significantly the physics accounted in the model. From the previous extreme value analysis, it can be inferred that 3 to 4 severe events during this winter, depending on the choice of buoy on site, show a return period between 1 and 5 year. More over, the sequence of significant wave height is not the only data of significant interest for the severity at stake, as time series of wave period (peak period and mean period T_{01}) reveal the high forcing levels recorded in the low frequency gravity band. This is particularly the case for the sea state generated by storm Hercules, striking from January 6th 2014 on Semrev site. Again, a quick analysis of IOWAGA integral parameters at global scales reveals that the combined H_s and T_p modelled for this event had not occurred since winter 1989-1990. A more detailed analysis of the spectral contents both in measurements and model output, and their evolution in time

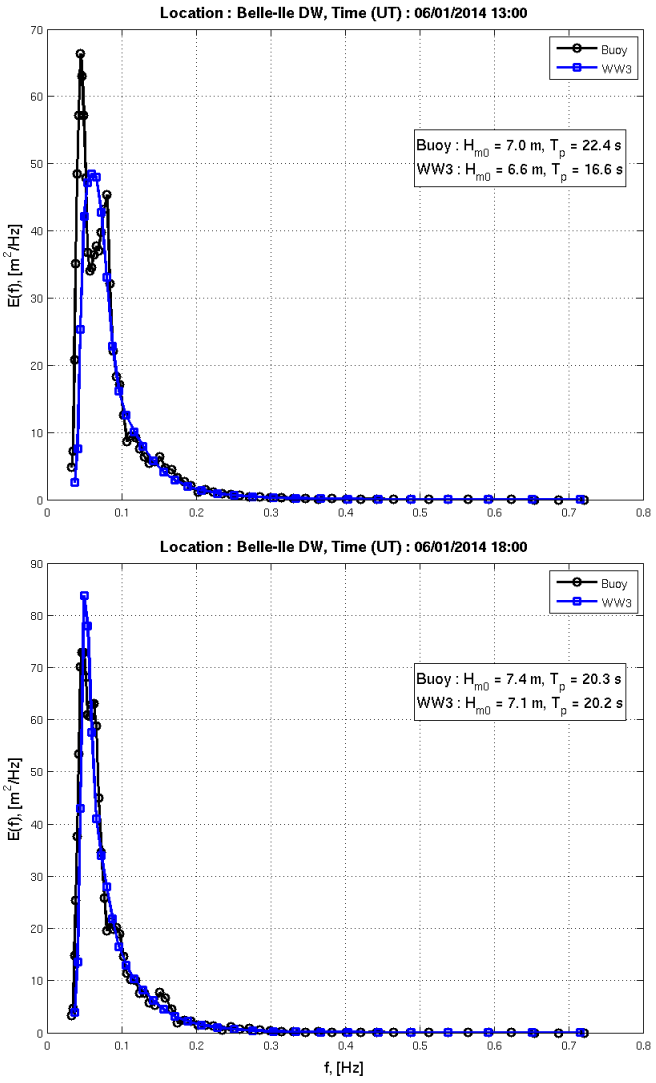

Fig. 8 - Comparison between observed and modelled spectra at Belle-Ile buoy, offshore of the test site, emphasizing misfit (13h00) and then proper accounting (18h00) of Hercules' long period components

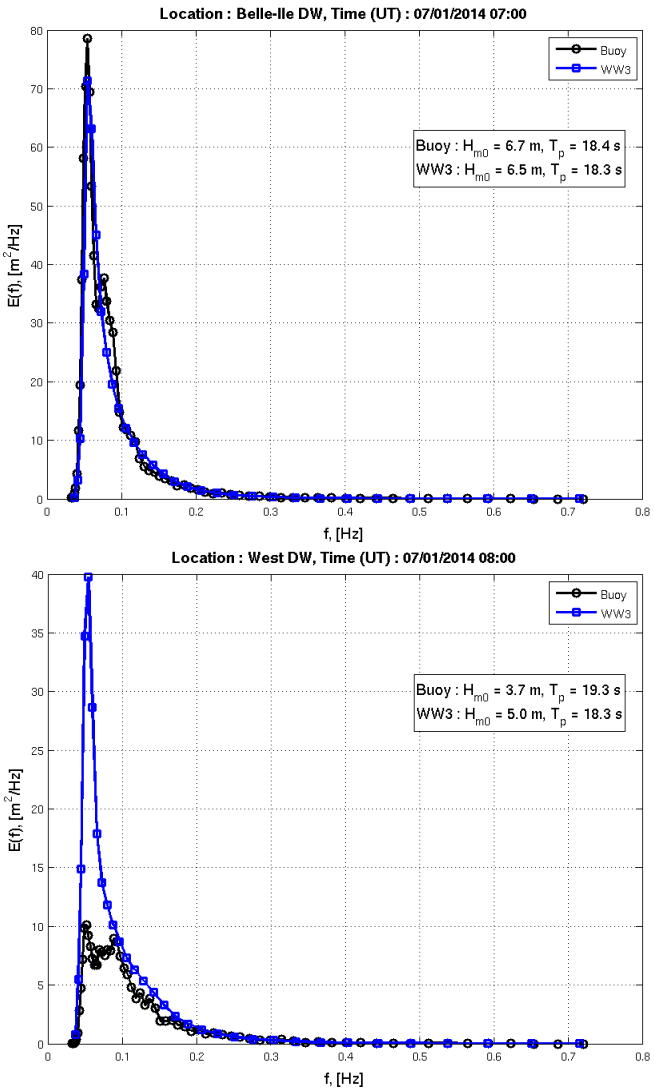

Fig. 9 - Comparison between observed and modelled spectra at Belle-Île and Semrev's West buoy showing for West Buoy an excess in modelled spectral density at peak frequency compared to buoy measurements

provides a proper overlook on the model capabilities in this strong swell conditions, which where until recently the least properly addressed in numerical wave models (Delpey et al. 2010). The time of arrival of the so-called frontrunners for this single event is under predicted by the model at the 3 measurement sites. Over a period of about 2 to 3 hours, the model shows a significant deficit in spectral density at low frequencies while the maximum measured peak period raises well above 20s. The bimodal shape of the 1D spectral measurements is not modelled at this stage either (Fig. 8). Also, when comparing measurements and models on site, the peakiness factor related to the measurement appears qualitatively significantly lower than the forecast of the model for those long periods components over the duration of the swell event, although the spectrum is well resolved offshore at Belle-Ile buoy for an equivalent record (Fig. 9). The significant wave height is also quite underestimated for this event. It is not clear at this stage if this enlightens the need for a more specific and refined dissipation term for low frequency

components, if buoys (both east and west buoys) are able to provide reliable measurement in those specific conditions, or if unresolved processes by the model are at stake. Complementary data through a pressure sensor deployed on site at the beginning of the winter and still recording for this event might enable in a future work to infer the reliability of the buoy measurements.

Several other comparisons have been conducted on the full 2D spectral data. At first, a qualitative comparison is provided here for the illustration purpose (Fig. 10 and Fig. 11). The directional records at Belle-Île buoy and associated MEM treatment, plotted here in frequency-azimuthal coordinates with a direction of origin convention, notably enables to discriminate low frequency components from the North-East sector. From the records, this is directly related to the amount of energy present in the incident sector and this is the record of the reflected low frequency components in the averaged normal direction to the iso-bathymetric contour, in the direct vicinity of Belle-Île cliffs. The misalignment in direction between wave components of opposed senses (i.e. incident West and supposedly reflected components from the East with a slight North component) discard mistreatment of the sense by the MEM method. Despite the accounting of a reflection term in the model formulation, model outputs don't exhibit such a component with an equivalent order of magnitude in spectral density. The spectral shape in both buoy and model outputs demonstrate a similar pattern. Several records at East and West buoy also show the same reflected components (not shown here). The discrepancies previously observed in the 1D spectral comparisons are illustrated in direction Fig. 11. The buoy records show a bimodal distribution, with a second peak at about two times the primary peak frequency and in the same direction. The model doesn't exhibit such a trend. Again, it is not clear at this stage which record would benefit from further refinements.

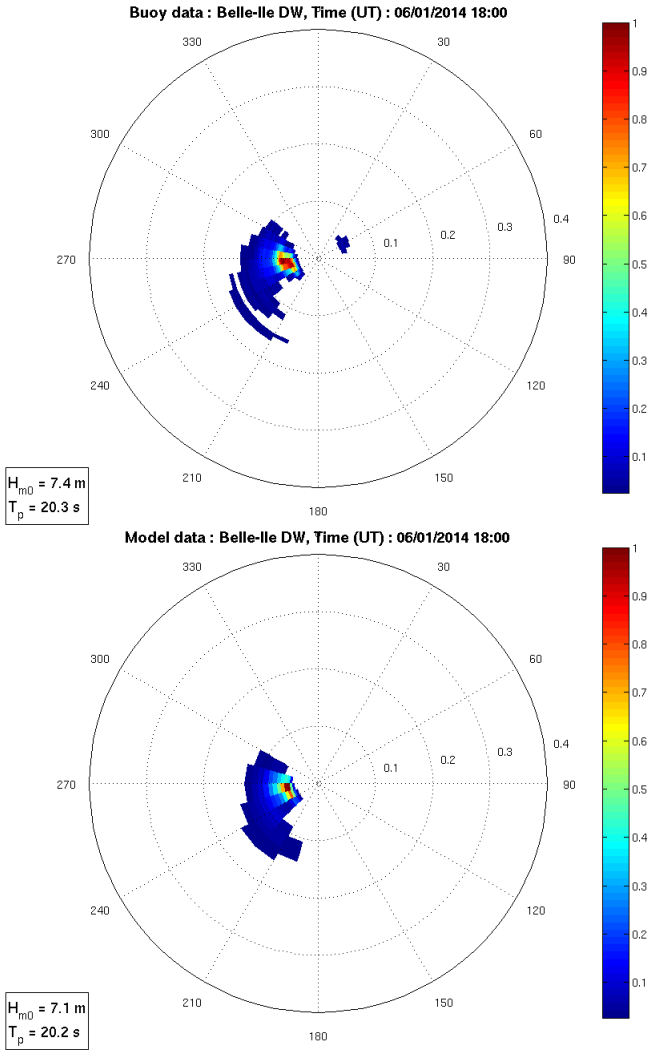

Fig. 10 - Comparison between observed and modelled 2D spectra at Belle-Ile buoy

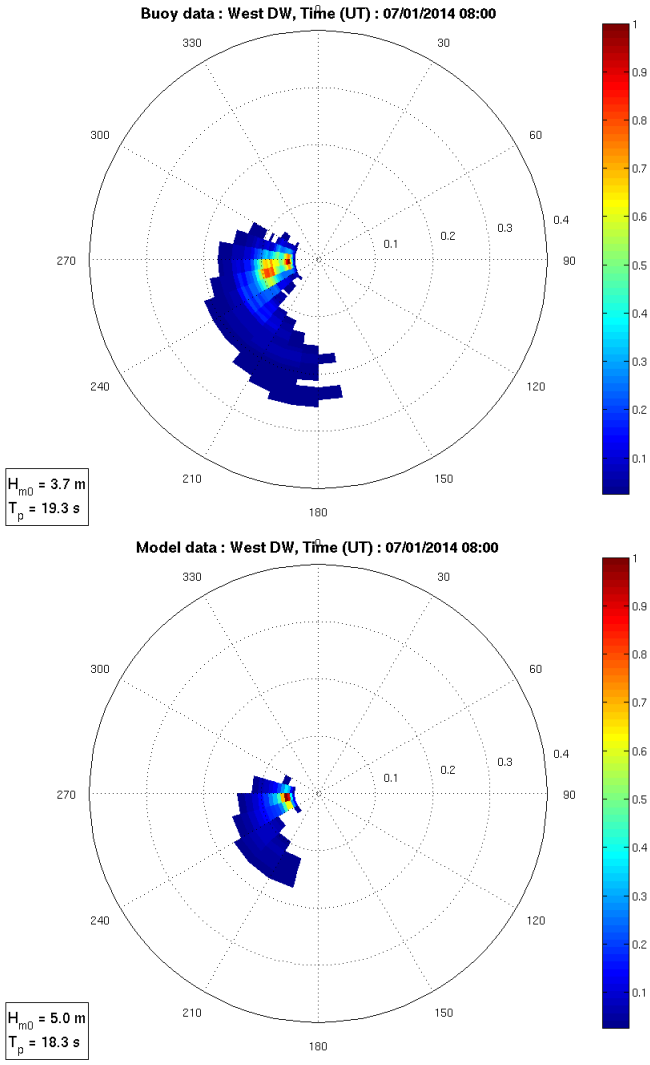

Fig. 11 - Comparison between observed and modelled 2D spectra at Semrev's West buoy

A more complete analysis of the time series of 2D spectra still demonstrates the new capabilities of the model chain, and the overall interest of the full 2D spectrum providing an overall proper estimate of the spectral pattern. The statistical estimators provided in equations (1) to (4) are applied to time series of spectral density $E(f,\theta)$, over 24h from 06/01/2014 14H00 to 07/01/2014 14H00 for the arrival of the most energetic low frequency components of the storm. The normalization of the estimators is however not performed independently for each time series, as it would not reflect the role of the relative error compared to the estimation of the total energy (i.e. a large error in a low energy bin over the period has a low impact on the result). The normalization is then achieved from the maximum energy bin of the time series, i.e.:

$$NRMSE\left(E\left(f_i,\theta_j\right)\right)= \sqrt{\frac{\sum_n\left(E_{obs}\left(f_i,\theta_j,t_n\right)-E_{\mathrm{mod}}\left(f_i,\theta_j,t_n\right)\right)^2}{\max_{i,j}\left(\sum_n E_{obs}\left(f_i,\theta_j,t_n\right)^2\right)}} \quad (6)$$

$$NB\left(E\left(f_i,\theta_j\right)\right)=\frac{\sum_n\left(E_{obs}\left(f_i,\theta_j,t_n\right)-E_{\mathrm{mod}}\left(f_i,\theta_j,t_n\right)\right)}{\max_{i,j}\left(\sum_n E_{obs}\left(f_i,\theta_j,t_n\right)\right)} \quad (7)$$

The SI, correcting the NRMSE from the Bias is calculated according to the same normalisation as in Eq. (6) applied to Eq. (4).

For the clarity of the following plot for spectral quantities, the estimators are blanked for spectral components below 1% of the maximum of the mean spectral energy over the 24h period (i.e. $\max_{i,j}\left(\bar{E}(f_i,\theta_j)\right)$). Such a treatment emphasizes the better prescription of the spectra at the offshore location (Belle-Ile) for this particular extremely low frequency and energetic event. While the SI (Fig. 12 and Fig. 14) are of the same order of magnitude for all three buoy, the SI corrects a larger relative bias (NB) to the NRMSE for the two buoy located on SEMREV (Fig. 13 and Fig. 15). There is a net negative bias located around the spectral area of the peaks during the period, related to the lower record compared to the prediction of the model. The bias is not as intense or homogeneous at the Belle-Île buoy. As long as the buoy record can be considered as a reference measurement, this could indicate that the shallow water dissipation of the long period swell is to be adjusted in the model.

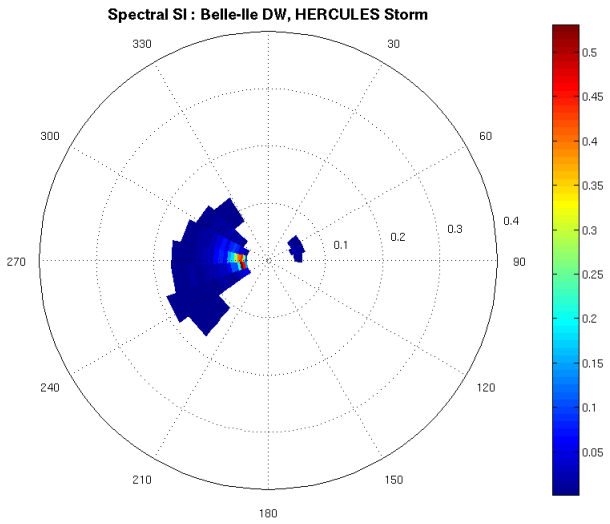

Fig. 12 - Distribution of the SI in directions and frequencies at Belle-Ile buoy

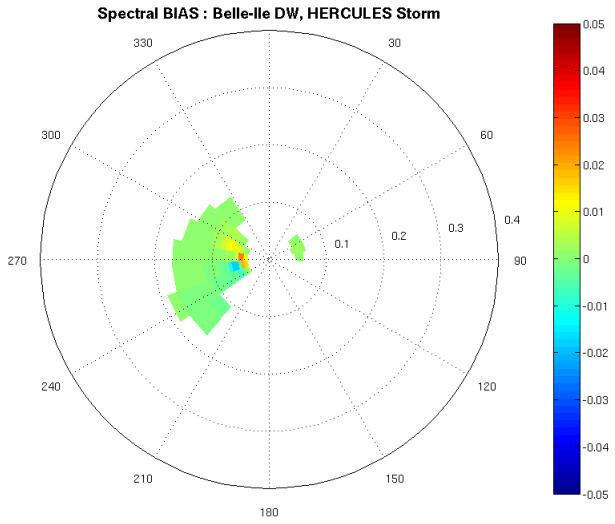

Fig. 13 - Distribution of Normalized Bias in directions and frequencies at Belle-Île buoy

More over, the comparison at both East and West buoys on site illustrates the homogeneity of the measurement and modelling (Fig. 14 and Fig. 15). The behaviour of the buoys as well as the modelling capabilities seem as a consequence quite consistent over the site. The extent of the SI in frequency is more pronounced in the comparisons at East and West buoys than at Belle-Île buoy. The plot of those quantities also illustrates the non-resolved mean reflected components, which are even above the 1% blanking threshold at the East Buoy.

Those not so common representations illustrate finally quite well the capabilities and flaws of the model for a specific extreme event in term of spectral properties. The application of this quite novel 2D-spectral environmental description of the sea states to various ocean engineering studies (e.g. power production, mooring loads on a floating platform, etc.) is well beyond the scope of the present paper, but the perspectives related to the use and analysis of this enriched and efficient new kind of hindcast are numerous.

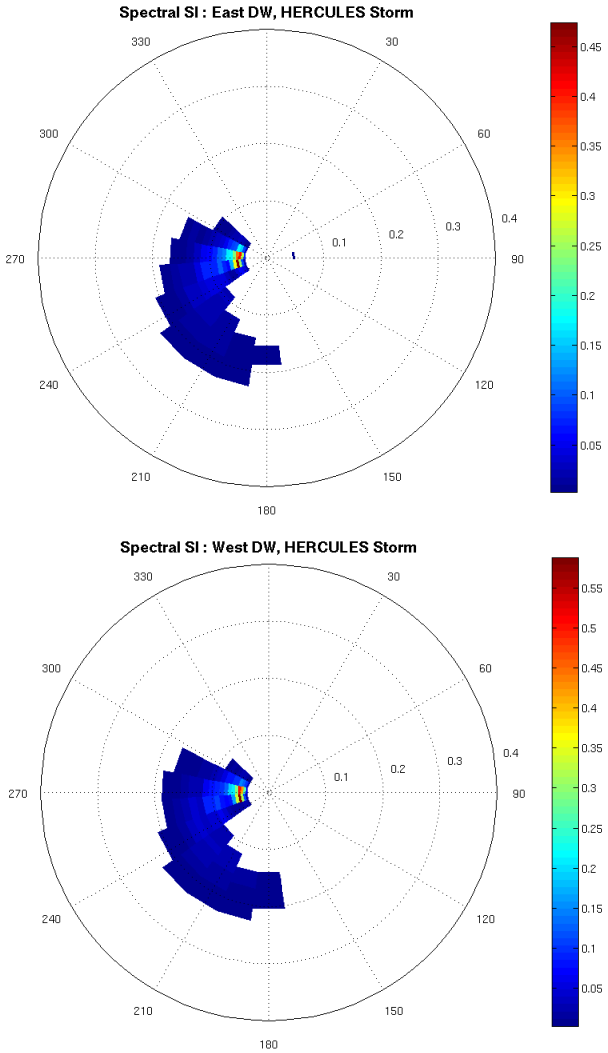

Fig. 14 - Distribution of the SI in directions and frequencies at East and West buoys

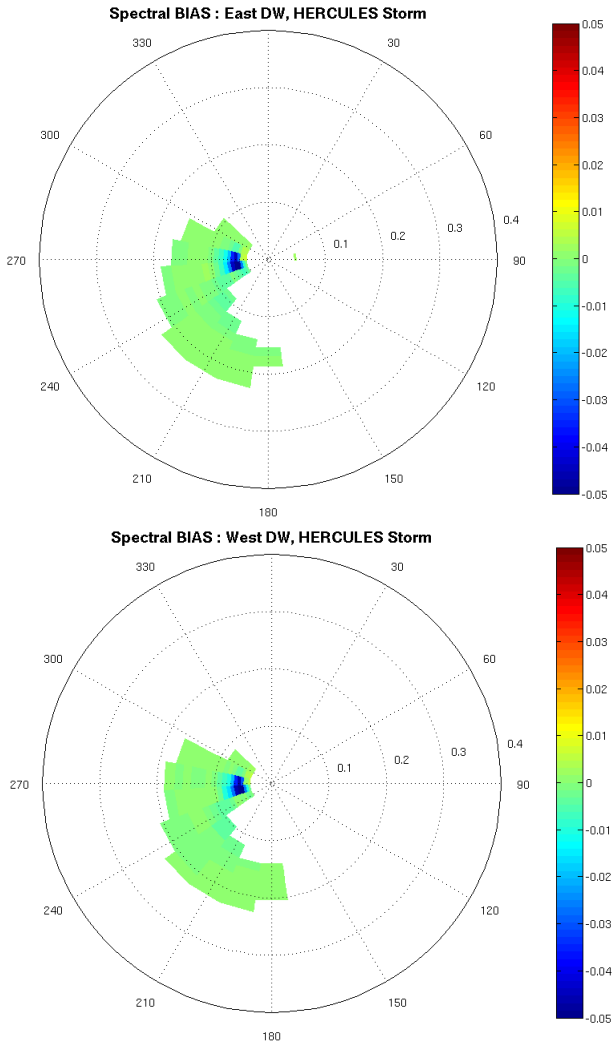

Fig. 15 - Distribution of the Normalized Bias in directions and frequencies at East and West buoys

VI. Conclusions

Some of the latest findings in term of model capabilities and derived products in regards to sea states have been applied in the specific context of the Semrev marine test site.

HOMERE, one of the latest and most detailed hindcast dataset for this area has been compared to local measurements, which demonstrates its overall best performances. Semrev's in-house complementary model chain, based on the same model and approach, and aimed at providing additional data, outside of the period already covered by HOMERE data set, has been demonstrated slightly less accurate on usual integral parameters. With a forcing accounted by a different wind datasets, different extents of domains, and a partial homogeneous accounting of the source term related to heterogeneous moveable bottom friction, the small discrepancies might come from several different causes.

The impact of the macro-tidal environment on the sea states on Semrev site has then been evaluated through sensitivity analysis in the in-house model. The variability induced by the accounting of currents fields and level variations seems to remain quite small and of the same order of magnitude as other natural sources. It is shown that for a spring tide period, the tidal forcing can cause variations for H_s up to 10%. The scores of the in house model benefit slightly from the additional forcing in term of scatter index and correlation to measurements. HOMERE data set seems to show a shift in the tidal modulation compared to measurements on this specific case in Semrev's area, which impairs its scores.

The spatial variability at the scale of the site dimensions is then studied taking advantage of the nearby measurements from East and West buoys on site, as well as from the locally refined modeling thanks to the irregular underlying grid of the in house model. It is shown that the variability between synchronized measurements causes up to 7% NRMS differences, when the model is able to provide the exact same trend, but with a less important difference of about 1.5%, to be related to the physical processes accounted by the model and at stake at the scale of the site.

An extreme value analysis and extrapolation is then conducted on the basis of HOMERE dataset extended from Semrev's in house data set for 2013 and 2014 years, through a

POT method combined to a GPD best fit. Some properties of the sequence of severe sea state conditions occurring during winter 2013 to 2014 are then inferred.

The capabilities and limitations of the Semrev model chain are finally illustrated for a specific severe event during this period and related to HERCULES atmospheric storm. For this quite specific and rare event combining large peak periods for the North Atlantic basin and high level of energy, (above 20s and nearly 5m of H_s on the SEMREV test site) a spectral description and comparison is enabled by the availability of both models and measurements. The overall performances of the hindcast dataset enlighten the potential use of the directional spectral description provided for the aim of refined analysis in numerous fields of ocean engineering.

ACKNOWLEDGMENT

The work presented here was supported by LHEEA Lab. at Ecole Centrale de Nantes, France, in the context of the scientific gathering LabexMer (Program “Investment for the future” grant ANR-10-LABX-19-01), and SEMREV test site.

The quality of the numerical model results owes much to the expertise, developments and products from research teams at LPO and DYNECO, Ifremer, Brest. The authors are more specifically grateful to F. Ardhuin (CNRS) for his kind help and advice. We thank the reviewers for their valuable comments and suggestions that have substantially improved our manuscript

REFERENCES

[1] Ardhuin, F., Chapron, B., & Collard, F. (2009). Observation of swell dissipation across oceans. *Geophys. Res. Lett. , 36*.

[2] Ardhuin, F., Rogers, E., Babanin, A. V., Filipot, J.-F., Magne, R., Roland, A., et al. (2010). Semi-empirical Dissipation Source Functions for Ocean Waves. Part I: Definition, Calibration, and Validation. *J. Phys. Oceanogr. , 40* (9), 1917-1941.

[3] Ardhuin, F., Roland, A., Dumas, F., Sentchev, A., Forget, P., Wolf, J., et al. (2012). Numerical wave modeling in conditions with strong currents: dissipation, refraction and relative wind . *J. Phys. Oceanogr. , 42*, 2101-2120.

[4] Berrisford, P., Kållberg, P., Kobayashi, S., Dee, D., Uppala, S., Simmons, A. J., et al. (2011). Atmospheric conservation properties in ERA-Interim. *Q.J.R. Meteorol. Soc. , 137*, 1381–1399.

[5] Boudiere, E., Maisondieu, C., Ardhuin, F., Accensi, M., Pineau-Guillou, L., & Lepesqueur, J. (2013). A suitable metocean hindcast database for the design of Marine energy converters. *International Journal of Marine Energy , 3-4*, e40-e52.

[6] Delpey, M. T., Ardhuin, F., Collard, F., & Chapron, B. (2010). Space-time structure of long ocean swell fields. *J. Geophys. Res. , 115* (C12).

[7] Dodet, G., Bertin, X., & Taborda, R. (2010). Wave climate variability in the North-East Atlantic Ocean over the last six decades. *Ocean Modeling , 31*, 120-131.

[8] Hasselmann, S., & Hasselmann, K. (1985). Computation and parameterizations of the nonlinear energy transfer in a gravity-wave spectrum. Part I: a new method for efficient computations of the exact nonlinear transfer. *J. Phys. Oceanogr.* (15), 1369–1377.

[9] Le Crom, I., Perignon, Y., Saulnier, J., & Berhault, C. (2013). Extreme Sea Conditions in Shallow Water: Estimations Based on In-Situ Measurements. *8*, p. 7. ASME.

[10] Pineau-Guillou, L., & al., e. *PREVIMER: Improvement of surge, sea level ans currents modelling.* Ifremer.

[11] Roland, A. (2008). *Development of WWM II: Spectral wave modelling on unstructured meshes.* Inst. of Hydraul. and Wave Resour. Eng., . Techn. Univer. Darmstadt, Germany.

[12] Roland, A., Cucco, A., Ferrarin, C., Hsu, T.-W., Liau, J.-M., Ou, S.-H., et al. (2009). On the development and verification of 2-D coupled wave-current model on unstructured meshes. *J. Mar. Syst.*

[13] Saha, S., & al., e. (2010). The NCEP Climate Forecast System Reanalysis . *Bul. Amer. Meteor. Soc. , 91* , 1015-1057.

[14] Saulnier, J., Soulard, T., Perignon, Y., Le Crom, I., & Babarit, A. (2013). About the Use of 3rd Generation Wave Prediction Models for Estimating the Performance of Wave Energy Converters in Coastal Regions. *EWTEC* . Aalbord.

[15] Thilleul, O., Berhault, C., Bossard, J., Cay, F., & Surmont, J.-c. P. Prediction of extreme responses for MRE structures : contribution of free surface CFD methods. *Proceedings 14 emes Journees de l'Hydrodynamique* (p. 2014). DGA Techniques Hydrodynamiques.

[16] Tolman, H., & et al. (2014). *User manual and system documentation of WAVEWATCH III version 4.18.* NOAA/NWS/NCEP. Hendrik Tolman.